

# Active Surface Tension of Cohesive Cell Colonies

Aaron F. Mertz,<sup>1</sup> Shiladitya Banerjee,<sup>2</sup> Yonglu Che,<sup>3,1</sup> Guy K. German,<sup>4</sup> Ye Xu (),<sup>4</sup> Callen Hyland,<sup>3</sup> M. Cristina Marchetti,<sup>2,5</sup> Valerie Horsley,<sup>3</sup> and Eric R. Dufresne<sup>4,6,1,7,\*</sup>

<sup>1</sup>*Department of Physics, Yale University, New Haven, Connecticut 06520, USA*

<sup>2</sup>*Department of Physics, Syracuse University, Syracuse, New York 13244, USA*

<sup>3</sup>*Department of Molecular, Cellular, and Developmental Biology,  
Yale University, New Haven, Connecticut 06520, USA*

<sup>4</sup>*Department of Mechanical Engineering & Materials Science,  
Yale University, New Haven, Connecticut 06520, USA*

<sup>5</sup>*Syracuse Biomaterials Institute, Syracuse University, Syracuse, New York 13244, USA*

<sup>6</sup>*Department of Chemical & Environmental Engineering,  
Yale University, New Haven, Connecticut 06520, USA*

<sup>7</sup>*Department of Cell Biology, Yale University, New Haven, Connecticut 06520, USA*

(Dated: May 28, 2022)

Little is known about how the mechanical properties of tissues emerge from interactions of multiple cells. To address this question, we measure traction stresses of cohesive colonies of 1–27 cells adherent to soft substrates. Traction stresses are generally localized at the periphery of the colony. For large colonies, we find that the total traction force scales linearly with the colony radius, not the number of cells. The observed scaling suggests the emergence of an active surface tension for adherent colonies of cohesive cells, of order  $10^{-3}$  N/m. A simple model of the cell colony as an active elastic medium coupled to the substrate captures the essential features of our data.

PACS numbers: 87.17.Rt, 87.19.R-, 68.03.Cd

Tissues have well defined mechanical properties such as elastic modulus [1]. They can also have properties unique to active systems, such as the homeostatic pressure recently proposed theoretically as a factor in tumor growth [2]. While the mechanical behavior of individual cells has been a focus of inquiry for more than a decade [3–6], the collective mechanics of groups of cells has only recently become a topic of investigation [7–15]. Yet, it is unknown how collective properties of tissues emerge from interactions of many cells.

In this Letter, we describe measurements of traction forces in colonies of cohesive epithelial cells adherent to a soft substrate. We find that the spatial distribution and magnitude of traction forces are more strongly influenced by the physical size of the colony than by the number of cells. We further show that, for large colonies, the total traction force,  $\mathcal{F}$ , that the cell colony exerts on the substrate is proportional to the equivalent radius,  $R$ , of the colony. This scaling suggests the emergence of a scale-free material property of the adherent tissue. The magnitude of this active surface tension is about  $10^{-3}$  N/m, much larger than the surface tension of a cell membrane. A simple physical model of adherent cell colonies as contractile elastic media captures the emergence of an active surface tension for large colonies.

To measure traction stresses that cells exert on their substrate, we used traction force microscopy (TFM) [16]. Our TFM setup consisted of a film of highly elastic silicone gel (Dow Corning Toray, CY52-276A/B) with thickness  $h_s = 27 \mu\text{m}$  on a rigid glass coverslip (Fig. 1A). Using bulk rheology, we estimated the Young's modulus of the gel to be 3 kPa. To quantify the gel deformation

during our experiments, our substrates contained two dilute layers of fluorescent beads (radius 100 nm, Invitrogen): one layer between the glass and gel and a second at height  $z_o = 24 \mu\text{m}$  above the coverslip [17]. To image the fluorescent beads, we used a spinning-disk confocal microscope (Andor Revolution, mounted on a Nikon Ti Eclipse inverted microscope with a  $40\times$  NA 1.3 objective). After determining bead positions using centroid analysis in MATLAB [18], we calculated the deformation of the substrate,  $u_i^s(\mathbf{r}, z_o)$ , across its stressed (with cells) and unstressed (with cells removed) states. In Fourier space, the deformation field is related to the traction forces at the surface of the substrate via linear elasticity,  $\sigma_{iz}^s(\mathbf{k}, h_s) = Q_{ij}(\mathbf{k}, z_o, h_s)u_j^s(\mathbf{k}, z_o)$ . Here,  $\sigma_{iz}^s(\mathbf{k}, h_s)$  and  $u_j^s(\mathbf{k}, z_o)$  are the Fourier transforms of the stress on the top surface and the displacements just below the surface, respectively. The tensor,  $Q$ , depends on the thickness and modulus of the substrate, the location of the beads, and the wave vector [17, 19]. We calculated the strain energy density,  $w(\mathbf{r}) = \frac{1}{2}\sigma_{iz}^s(\mathbf{r}, h_s)u_i^s(\mathbf{r}, h_s)$ , which represents the work per unit area performed by the cell colony to deform the elastic substrate [20]. The deformation on the surface was determined using  $u_i^s(\mathbf{k}, h_s) = Q_{ij}^{-1}(\mathbf{k}, h_s, h_s)Q_{jk}(\mathbf{k}, z_o, h_s)u_k^s(\mathbf{k}, z_o)$ .

Primary mouse keratinocytes were isolated and cultured as described in [21]. We plated keratinocytes on fibronectin-coated TFM substrates. After the cells proliferated to the desired colony sizes over 6–72 hr, we raised the concentration of  $\text{CaCl}_2$  in the growth medium from 0.05 mM to 1.5 mM. After 18–24 hr in the high-calcium medium, cadherin-based adhesions formed between adjacent keratinocytes, which organized themselves into cohe-

sive single-layer cell colonies [22, 23]. After imaging the beads in their stressed positions, we removed the cells by applying proteinase K and imaged the beads in their unstressed positions.

Stress fields and strain energy densities for representative colonies of one, two, and twelve keratinocytes are shown in Fig. 1. Traction stresses generically point inward, indicating that the colonies are adherent and contractile. Regions of high strain energy appear to be localized primarily at the periphery of the single- or multi-cell colony. For single cells, these findings are consistent with myriad previous reports on the mechanics of isolated, adherent cells [24, 25]. Recent reports have also observed the localization of high stress in the periphery of small cell colonies on micropatterned substrates [26] and at edges of cell monolayers [7, 8, 13]. To visualize cell-cell and cell-matrix adhesions, we immunostained multi-cell colonies for E-cadherin and zyxin. Additionally, we stained the actin cytoskeleton with phalloidin. Actin stress fibers were concentrated at colony peripheries and usually terminated with focal adhesions, as indicated by the presence of zyxin at the fibers' endpoints. In contrast, E-cadherin was localized at cell-cell junctions, typically alongside small actin fibers. Despite differences in the architecture of the relevant proteins, the stresses and strain energy distributions are remarkably similar in the single-cell and multi-cell colonies.

To explore these trends, we measured traction stresses of 50 cohesive colonies of 1–27 cells. For each colony, we defined an equivalent radius,  $R$ , as the radius of a disk with the same area. The equivalent radii ranged from 20 to 200  $\mu\text{m}$ . We calculated the average strain energy density as a function of distance,  $\Delta$ , from the colony edge (Fig. 2 inset). Figure 2 shows the normalized strain energy profiles,  $\bar{w}(\Delta)/\bar{w}(0)$ , of all 50 colonies. Usually, the strain energy density was largest near the colony edge ( $\Delta = 0$ ). Because of the finite spatial resolution of our implementation of TFM, we measured some strain energy outside colony boundaries ( $\Delta < 0$ ).

Next, we examined how global mechanical activity changes with the cell number and geometrical size of the colony. As in previous studies, we calculated the “total traction force” [27, 28],

$$\mathcal{F} = \int dA \sqrt{(\sigma_{xz}^s)^2 + (\sigma_{yz}^s)^2}, \quad (1)$$

exerted by the cell colony onto the substrate. This quantity is meaningful when stresses have radial symmetry and are localized at the colony edge, which is the case for the majority of colonies in this study. We observed a strong positive correlation between equivalent radius and total force over the range of keratinocyte colonies examined (Fig. 3). Similar trends have been seen for isolated cells over a smaller dynamic range of sizes [27–30]. We see no systematic differences in  $\mathcal{F}$  for colonies of the same size having different numbers of cells, suggesting

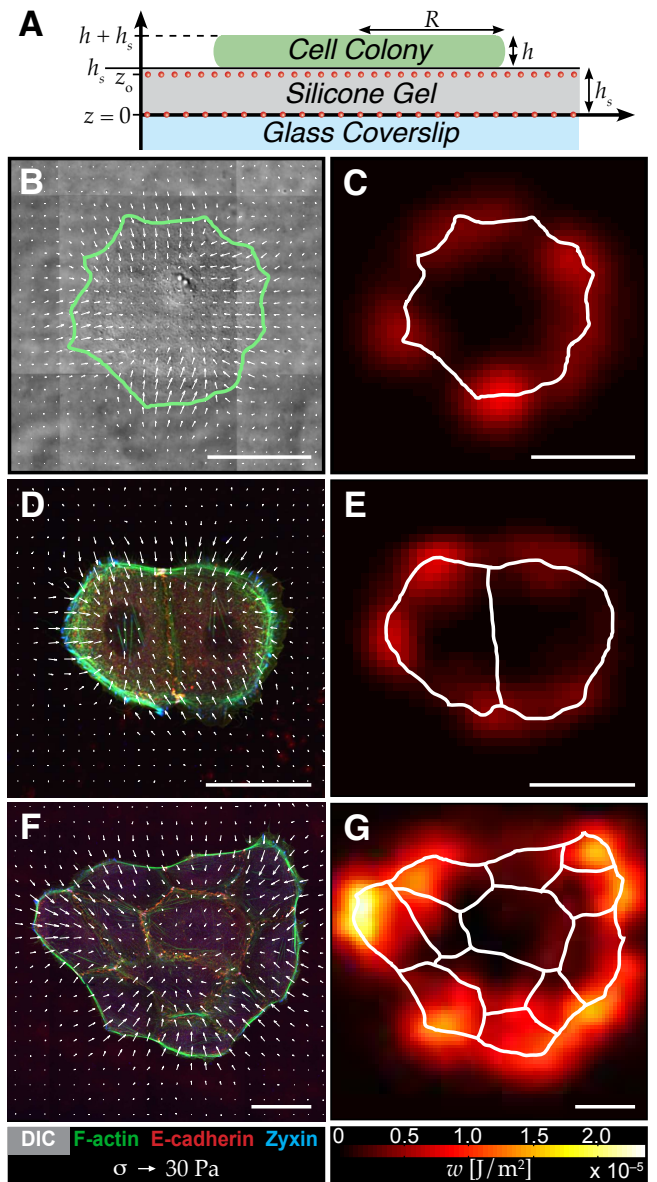


FIG. 1: (color online) Traction stresses and strain energies for colonies of cohesive keratinocytes. (A) Schematic of experimental setup (not to scale) with a cell colony adherent to an elastic substrate embedded with two dilute layers of fluorescent beads. (B, D, F) Stress distribution,  $\sigma$ , and (C, E, G) strain energy,  $w$ , for a representative single cell, pair of cells, and colony of 12 cells. Stress distribution is overlaid on a DIC image (B) or images of immunostained cells (D, F). Solid lines in (A–C, E, G) mark cell boundaries. For clarity, only half of the calculated stresses are shown in (B, D) and one-quarter of the stresses in (F). Scale bars in (B–G) represent 50  $\mu\text{m}$ .

that cohesive cells cooperate to create a mechanically coherent unit. Cohesive colonies appear to act like large single cells, suggestive of the behavior of syncytia, which are large, multinucleated cells that coordinate biological function within one membrane [31].

These results suggest a scaling relationship between

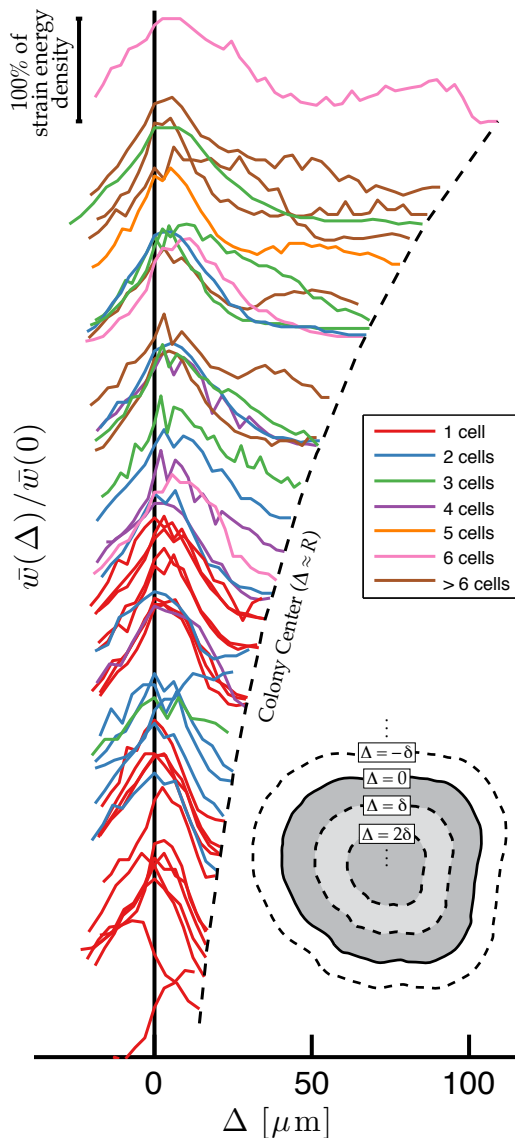


FIG. 2: (color online) Spatial distribution of strain energy for colonies of different size. Each curve represents a colony's measured strain energy density as a function of distance from the edge of the colony,  $\Delta$ . For clarity, the profiles are spaced vertically according to the size of the colony. Each profile terminates at the point where the inward erosion of the outer edge covers the entire area of the colony, at  $\Delta \approx R$ . The erosion proceeds in discrete steps of size  $\delta$ , as illustrated in the inset.

mechanical output of cell colonies and their geometrical size, independent of the number of cells:  $\mathcal{F} \sim R^\lambda$ . The scaling exponent,  $\lambda$ , appears to be approach 1 for large colonies. For smaller colonies, the scatter is greater, and the exponent could be between 2 and 3. We hypothesize that the transition to an apparently consistent exponent for the large colonies is equivalent to the emergence of a scale-free material property of a tissue, defined by the ratio  $\mathcal{F}/(2\pi R) = (8 \pm 2) \times 10^{-4}$  N/m, with dimensions of surface tension.

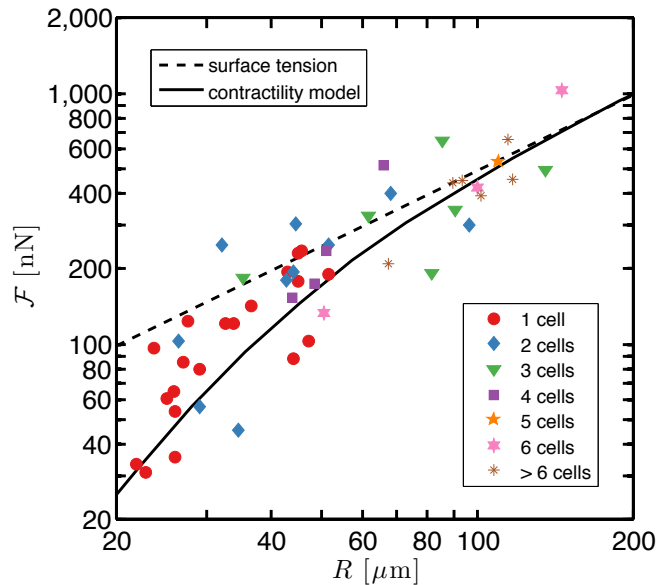


FIG. 3: (color online) Mechanical output of keratinocyte colonies versus geometrical size. Total force transmitted to the substrate by the cell colonies, defined in Eq. (1), is plotted as a function of the equivalent radius of the colonies. The dashed line represents scaling expected for surface tension,  $\mathcal{F} \sim R$ . The solid line shows the a fit of the data to the minimal contractility model in Eq. (8).

Just as intermolecular forces yield the condensation of molecules into a dense phase, cohesive interactions between cells, mediated by cadherins, cause them to form dense colonies. For large ensembles of molecules, these molecular interactions are manifest as an emergent material property called surface tension. Surface tension has units of energy per area and describes the free energy penalty for creating an interface between two phases. An effective surface tension of cell agglomerates has been invoked to explain cell sorting and embryogenesis [32]. Previous measurements of non-adherent aggregates of cohesive cells reported effective surface tensions between 2 and 20 mN/m [33, 34]. It is tempting to think of the adherent colonies studied here as aggregates of cohesive cells that have wet the surface. Indeed, when matter wets a surface, the forces are localized at the contact line [35, 36]. This analogy describes the concentration of forces at the colony boundary and perhaps the correlation of traction stresses to the curvature of the colony edge [7]. However, the origins of the effective surface tension of cohesive cells are distinct from conventional surface tension. Indeed, the surface tension of a cell membrane, about  $3 \times 10^{-6}$  J/m<sup>2</sup> [37], is orders of magnitude smaller than the effective surface tension of the adherent colony. It has recently been suggested that the surface tension of developing embryos is determined by contributions from cell-cell adhesions and the contraction of acto-myosin networks [32]. To distinguish the effective

surface tension due to active processes from the familiar surface tension defined in thermodynamic equilibrium, we call it “active surface tension”.

To elucidate the origins of active surface tension in these experiments, we consider a minimal model proposed recently to describe cell–substrate interactions [38, 39]. We describe a cohesive colony as an active elastic disk of thickness  $h$  and radius  $R$  (Fig. 1A). The mechanical properties of the cell colony are assumed to be homogeneous and isotropic with Young’s modulus  $E$  and Poisson’s ratio  $\nu$ . Acto-myosin contractility is modeled as a contribution to the local pressure, linearly proportional to the chemical potential difference,  $\Delta\mu$ , between ATP and its hydrolysis products [40]. The constitutive equations for the stress tensor,  $\sigma_{ij}$ , of the colony are then given by

$$\sigma_{ij} = \frac{E}{2(1+\nu)} \left[ \frac{2\nu}{1-2\nu} \nabla \cdot \mathbf{u} + \partial_i u_j + \partial_j u_i \right] + \delta_{ij} \zeta \Delta\mu, \quad (2)$$

where  $\mathbf{u}$  is the displacement field of the cell colony and  $\zeta > 0$  a material parameter that controls the strength of the active pressure,  $\zeta \Delta\mu$ . Mechanical equilibrium requires that  $\partial_j \sigma_{ij} = 0$ .

We use cylindrical coordinates and assume in-plane rotational symmetry. The top surface is stress-free,  $\sigma_{rz}|_{z=h+h_s} = 0$ , and we employ a simplified coupling of the colony to substrate. Ignoring all nonlocal effects arising from the substrate elasticity,  $\sigma_{rz}|_{z=h_s} = Y u_r(z=h_s) \approx Y \bar{u}_r$ . Here,  $u_r$  is the radial component of the displacement field, the bar denotes  $z$ -averaged quantities, and the rigidity parameter,  $Y$ , describes the coupling of the contractile elements of the cell to the underlying substrate. The local equivalence of stress and displacement is accurate only when the substrate thickness is much smaller than the characteristic length scale of the stress distribution or when the cells are on substrates of soft posts [30]. On a smooth surface,  $Y$  can be estimated as  $k_{\text{eff}} \rho_f$ , where  $\rho_f$  is the density of focal adhesions and  $k_{\text{eff}}$  is the effective stiffness of a coupled focal adhesion and elastic substrate, which could be modeled as two springs in series.

With these assumptions, the equation of force-balance simplifies to

$$[\partial_r(r\bar{\sigma}_{rr}) - \bar{\sigma}_{\theta\theta}] / r = Y \bar{u}_r / h. \quad (3)$$

Combining Eqs. (2) and (3), we find the governing equation for the radial deformation,  $u_r$ :

$$r^2 \partial_r^2 u_r + r \partial_r u_r - (1 + r^2 / \ell_p^2) u_r = 0, \quad (4)$$

where the penetration length,  $\ell_p$ , is given by

$$\ell_p^2 = \frac{E(1-\nu)h}{Y(1+\nu)(1-2\nu)}. \quad (5)$$

The solution of Eq. (4) with boundary conditions  $u_r(r=0) = 0$  and  $\sigma_{rr}(r=R) = 0$  can be expressed in terms of

modified Bessel functions as

$$u(r) = -\zeta \Delta\mu \left[ \frac{(1+\nu)(1-2\nu)}{E(1-\nu)} \right] R I_1(\beta r/R) A(\beta), \quad (6)$$

with  $\beta = R/\ell_p$  and

$$[A(\beta)]^{-1} = \beta I_0(\beta) - \left( \frac{1-2\nu}{1-\nu} \right) I_1(\beta). \quad (7)$$

As in our experiments, the resulting deformations and traction stresses are localized near the colony edge (Fig. 2). To compare quantitatively to experiments, we calculate the total force,

$$\mathcal{F}(R) = 2\pi Y \left| \int_0^R r dr u_r(r) \right|. \quad (8)$$

In the large colony limit, for  $R \gg \ell_p$ , we find

$$\mathcal{F}(R) \simeq 2\pi \zeta \Delta\mu h R \sim R, \quad (9)$$

yielding the anticipated linear growth of total force for large colonies. In this limit, the contractile active pressure dominates over internal elastic stresses and underlies the observed active surface tension.

The theory matches the scaling of the data reasonably well with  $\ell_p = 16 \mu\text{m}$  and active surface tension  $\zeta \Delta\mu h \approx 8 \times 10^{-4} \text{N/m}$ , as shown by the solid line in Fig. 3. The penetration length,  $\ell_p$ , describes the localization of stresses near the boundary of the cell colony and is comparable to the spatial resolution of our measurements. The fitted value of the effective surface tension implies  $\zeta \Delta\mu \approx 4 \text{kPa}$  for a cell colony of thickness  $h \approx 0.2 \mu\text{m}$ . This value is consistent with that inferred from experiments in crawling keratocytes [41]. We can estimate the active pressure by assuming  $\zeta \Delta\mu \approx \rho_m k_m \Delta_m$ , where  $\rho_m$  is the areal density of bound myosin motors,  $k_m$  the stiffness of motor filaments and  $\Delta_m$  their average stretch. Using  $k_m \approx 1 \text{pN/nm}$ ,  $\Delta_m \approx 1 \text{nm}$ , and  $\rho_m \approx 10^3 \mu\text{m}^{-2}$ , we find  $\zeta \Delta\mu \approx 1 \text{kPa}$  [42, 43].

In conclusion, we observed the emergence of an active surface tension for colonies of cohesive cells adherent to soft substrates. We found that a simple physical model of cohesive colonies as adherent contractile disks captures the essential physics. It is intriguing that a model of a cell colony with homogenous and isotropic properties is so successful when the morphology of the underlying acto-myosin networks within the colony are patently anisotropic and heterogeneous (Fig. 1). Experiments measuring the active surface tension of colonies on substrates with different stiffnesses and with molecular perturbations that affect the contractility of acto-myosin networks will be particularly valuable to reveal the limitations of the current model. From a cell biology perspective, it will be essential to determine the molecular mechanisms that regulate a colony’s active surface tension.

We are grateful to Paul Forscher and Margaret L. Gardel for helpful discussions. This work was supported by an NSF Graduate Research Fellowship to A.F.M. and C.H., NSF grants to E.R.D. (DBI-0619674) and M.C.M. (DMR-0806511 and DMR-1004789), NIH grants to V.H. (AR054775 and AR060295), as well as support to E.R.D. from Unilever.

---

\* eric.dufresne@yale.edu

- [1] D. Discher, P. Janmey, and Y. Wang, *Science* **310**, 1139 (2005).
- [2] M. Basan, T. Risler, J. Joanny, X. Sastre-Garau, and J. Prost, *HFSP Journal* **3**, 265 (2009).
- [3] J. Lee, M. Leonard, T. Oliver, A. Ishihara, and K. Jacobson, *The Journal of Cell Biology* **127**, 1957 (1994).
- [4] R. Ananthakrishnan and A. Ehrlicher, *International Journal of Biological Sciences* **3**, 303 (2007).
- [5] V. Vogel and M. Sheetz, *Nature Reviews Molecular Cell Biology* **7**, 265 (2006).
- [6] M. Gardel, B. Sabass, L. Ji, G. Danuser, U. Schwarz, and C. Waterman, *The Journal of Cell Biology* **183**, 999 (2008).
- [7] C. M. Nelson, R. P. Jean, J. L. Tan, W. F. Liu, N. J. Sniadecki, A. A. Spector, and C. S. Chen, *Proceedings of the National Academy of Sciences of the United States of America* **102**, 11594 (2005).
- [8] O. du Roure, A. Saez, A. Buguin, R. Austin, P. Chavrier, P. Silberzan, and B. Ladoux, *Proceedings of the National Academy of Sciences of the United States of America* **102**, 14122 (2005).
- [9] X. Trepate, M. Wasserman, T. Angelini, E. Millet, D. Weitz, J. Butler, and J. Fredberg, *Nature Physics* **5**, 426 (2009).
- [10] T. Angelini, E. Hannezo, X. Trepate, J. Fredberg, and D. Weitz, *Physical Review Letters* **104**, 168104 (2010).
- [11] A. Khalil and P. Friedl, *Integrative Biology* **2**, 568 (2010).
- [12] Z. Liu, J. Tan, D. Cohen, M. Yang, N. Sniadecki, S. Ruiz, C. Nelson, and C. Chen, *Proceedings of the National Academy of Sciences of the United States of America* **107**, 9944 (2010).
- [13] A. Saez, E. Anon, M. Ghibaudo, O. du Roure, J. Di Meglio, P. Hersen, P. Silberzan, A. Buguin, and B. Ladoux, *Journal of Physics: Condensed Matter* **22**, (2010).
- [14] D. Tambe, C. Hardin, T. Angelini, K. Rajendran, C. Park, X. Serra-Picamal, E. Zhou, M. Zaman, J. Butler, D. Weitz, et al., *Nature Materials* **10**, 469 (2011).
- [15] V. Maruthamuthu, B. Sabass, U. Schwarz, and M. Gardel, *Proceedings of the National Academy of Sciences of the United States of America* **108**, 4708 (2011).
- [16] M. Dembo and Y. Wang, *Biophysical Journal* **76**, 2307 (1999).
- [17] Y. Xu, W. Engl, E. Jerison, K. Wallenstein, C. Hyland, L. Wilen, and E. Dufresne, *Proceedings of the National Academy of Sciences of the United States of America* **107**, 14964 (2010).
- [18] J. Crocker and D. Grier, *Journal of Colloid and Interface Science* **179**, 298 (1996).
- [19] J. del Alamo, R. Meili, B. Alonso-Latorre, J. Rodriguez-Rodriguez, A. Aliseda, R. Firtel, and J. Lasheras, *Proceedings of the National Academy of Sciences of the United States of America* **104**, 13343 (2007).
- [20] J. Butler, I. Tolić-Nørrelykke, B. Fabry, and J. Fredberg, *American Journal of Physiology – Cell Physiology* **282**, C595 (2002).
- [21] Y. Barrandon and H. Green, *Proceedings of the National Academy of Sciences of the United States of America* **84**, 2302 (1987).
- [22] E. O’Keefe, R. Briggaman, and B. Herman, *Journal of Cell Biology* **105**, 807 (1987).
- [23] A. Vaezi, C. Bauer, V. Vasioukhin, and E. Fuchs, *Developmental Cell* **3**, 367 (2002).
- [24] H.-B. Wang, M. Dembo, S. Hanks, and Y.-I. Wang, *Proceedings of the National Academy of Sciences of the United States of America* **98**, 11295 (2001).
- [25] N. Wang, E. Ostuni, G. Whitesides, and D. Ingber, *Cell Motility and the Cytoskeleton* **52**, 97 (2002).
- [26] R. Krishnan, D. Klumpers, C. Park, K. Rajendran, X. Trepate, J. van Bezu, V. van Hinsbergh, C. Carman, J. Brain, J. Fredberg, et al., *American Journal of Physiology – Cell Physiology* **300**, C146 (2011).
- [27] J. Califano and C. Reinhart-King, *Cellular and Molecular Bioengineering* **3**, 68 (2010).
- [28] J. Fu, Y. Wang, M. Yang, R. Desai, X. Yu, Z. Liu, and C. Chen, *Nature Methods* **7**, 733 (2010).
- [29] I. Tolić-Nørrelykke and N. Wang, *Journal of Biomechanics* **38**, 1405 (2005).
- [30] J. Tan, J. Tien, D. Pirone, D. Gray, K. Bhadriraju, and C. Chen, *Proceedings of the National Academy of Sciences of the United States of America* **100**, 1484 (2003).
- [31] B. Alberts, A. Johnson, J. Lewis, M. Raff, K. Roberts, and P. Walter, *Molecular Biology of the Cell* (Garland Science, 2007), 5th ed.
- [32] M. Manning, R. Foty, M. Steinberg, and E. Schoetz, *Proceedings of the National Academy of Sciences of the United States of America* **107**, 12517 (2010).
- [33] R. Foty, G. Forgacs, C. Pfeleger, and M. Steinberg, *Physical Review Letters* **72**, 2298 (1994).
- [34] R. Foty, C. Pfeleger, G. Forgacs, and M. Steinberg, *Development* **122**, 1611 (1996).
- [35] P.-G. de Gennes, F. Brochard-Wyart, and D. Quèrè, *Capillarity and wetting phenomena: drops, bubbles, pearls, waves* (Springer-Verlag, New York, 2004).
- [36] E. Jerison, Y. Xu, L. Wilen, and E. Dufresne, *Physical Review Letters* **106**, 186103 (2011).
- [37] F. Hochmuth, J. Shao, J. Dai, and M. Sheetz, *Biophysical Journal* **70**, 358 (1996).
- [38] S. Banerjee and M. Marchetti, *Europhysics Letters* **96**, 28003 (2011).
- [39] C. Edwards and U. Schwarz, *Physical Review Letters* **107**, 128101 (2011).
- [40] K. Kruse, J. Joanny, F. Jülicher, J. Prost, and K. Sekimoto, *The European Physical Journal E: Soft Matter and Biological Physics* **16**, 5 (2005).
- [41] K. Kruse, J. Joanny, F. Jülicher, and J. Prost, *Physical Biology* **3**, 130 (2006).
- [42] S. Günther and K. Kruse, *New Journal of Physics* **9**, 417 (2007).
- [43] S. Banerjee, T. Liverpool, and M. Marchetti, *Europhysics Letters* **96**, 58004 (2011).